ChemComm

Degradable Optical Resonators as In Situ Microprobes for Microscopy-Based Observation of Enzymatic Hydrolysis

Journal:	*ChemComm*
Manuscript ID	CC-COM-10-2022-005597.R1
Article Type:	Communication

COMMUNICATION

Degradable Optical Resonators as *In Situ* Microprobes for Microscopy-Based Observation of Enzymatic Hydrolysis

Received 00th January 20xx,
Accepted 00th January 20xx

DOI: 10.1039/x0xx00000x

Akihide Takeuchi,[a] Wey Yih Heah,[a] Yohei Yamamoto *[a] and Hiroshi Yamagishi *[a]

Optical resonators work as precise physical and chemical sensors. Here, we assemble a whispering gallery mode resonator from a natural polymer, fibroin protein, and successfully observe its catalytic degradation reaction as a spectral shift. This methodology will contribute to the precise *in situ* observation of biological reactions by optical microscopy.

Hydrolysis of insoluble polymers is an essential chemical event in several biological activities, such as metabolism of cells and phagocytosis of microparticles.[1, 2] Hydrolysis is also valuable in a series of industrial processes, such as fermentation of foods and purification of sewerage.[3-6] Hydrolysis reactions, in most cases, take place at the interface between a solid and water and are facilitated by chemical catalysts or enzymes adsorbed on the surface. To analyse the kinetics of such heterogeneous reactions, researchers have conventionally measured the weight of the solid components that are extracted in the middle of the reactions.[7-10] Typically, a portion of the reaction mixture is sampled, and the weight and appearance of the residual solid component is measured after washing and drying. This methodology is straightforward but relatively inaccurate and takes a long time (a few days or months) until the weight loss exceeds the error of the measurement.

To achieve higher precision, several advanced analytical techniques have been proposed. A quartz crystal microbalance (QCM) is highly precise in measurements of the weight loss of a thin polymer film evenly deposited onto an electrode.[11, 12] High-performance liquid chromatography, gel permeation chromatography, and gel electrophoresis are typical quantitative techniques to quantitate and identify the chemical structure of reaction products dissolved in aqueous media.[13-15] The precision improves drastically with these methods, but they still require sampling and are applicable only to macroscopic substances. Therefore, these methods are incompatible with optical microscopy, which is an essential tool for a series of biological and environmental studies. We anticipate that an *in situ* analytical method that is compatible with a microscope will contribute greatly to in-depth studies on hydrolysis at the microscale. A methodology using a scanning probe microscope reported by Igarashi and coworkers can detect morphological changes at the surface of cellulose.[16] However, probe microscopes are not quantitative and usually require a complex apparatus and extensive optimization of the observation conditions. Moreover, probe microscopy is still difficult to integrate with optical microscopy, prohibiting the integrated analysis of cellular and enzymatic events at the microscale.

Our previous works on molecular assembly and the associated optical measurements provided a potential strategy

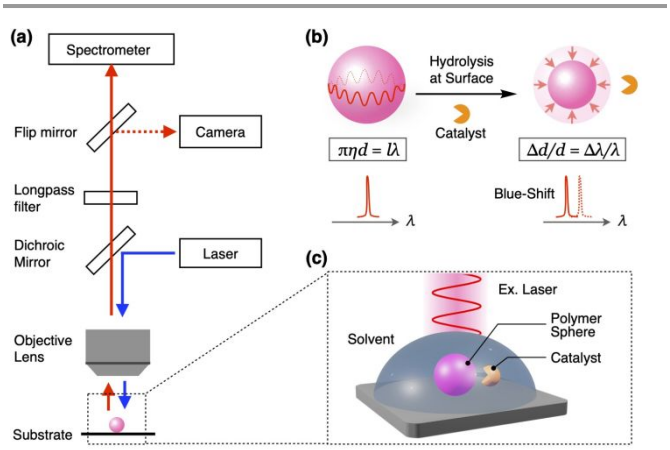

Fig. 1 (a) A schematic representation of the microscopic photoluminescence spectroscopy (μ-PL) for the *in situ* monitoring of the hydrolysis kinetics of a polymer. (b) A schematic representation of the quantitative measurements of the hydrolysis reaction based on the spectral shift of the resonance peaks.

[a] *Department of Materials Science, Institute of Pure and Applied Sciences, and Tsukuba Research Center for Energy Materials Science (TREMS) University of Tsukuba 1-1-1 Tennodai, Tsukuba, Ibaraki 305-8573, Japan.*

† Electronic Supplementary Information (ESI) available: [details of any supplementary information available should be included here]. See DOI: 10.1039/x0xx00000x

to achieve quantitative analysis of the hydrolysis kinetics with optical microscopes, namely, observation of the decrease in size of polymer particles as a spectral shift (Fig. 1). We reported a versatile self-assembly-based synthetic method for micrometre-scale spherical particles (MS) from various types of organic polymers.[17] This method is applicable not only to synthetic polymers but also to biological polymers such as fibroin proteins of silkworms.[18] These MSs confine light via total internal reflection at the particle surface and thus work as active whispering gallery mode (WGM) optical resonators.[19-22] We demonstrated that these MSs work as highly sensitive chemical and physical sensors at the microscale.[23, 24] The periodic resonance peaks underwent a spectral shift towards the shorter or longer wavelength region in response to changes in the refractive index and the radius of the sphere, and the change could be traced with high precision due to the sharpness of the resonance peaks (Fig. 1b). In the present study, we hypothesize that this method may enable the detection of the heterogeneous hydrolysis reaction progress as a spectral shift of the resonance peaks.

We chose natural silk fibroin protein produced by silkworms (*Bombyx mori*, Fig. 2a) as a model compound that readily decomposes under aqueous conditions. We previously reported the synthesis of microspherical particles from fibroin proteins (**MS$_{silk}$**) and their optical resonance properties.[18] According to that report, **MS$_{silk}$** was prepared and doped with Nile Red as a fluorescent dye. **MS$_{silk}$** was drop-cast onto a quartz substrate for optical microscopy (OM) and fluorescence microscopy (FM) observations and onto a silicon substrate for scanning electron microscopy (SEM) observations. As visualized by SEM and OM, the morphology of **MS$_{silk}$** was highly spherical, with an average diameter of 2.9 μm (Fig. 2b, d, and Fig. S1). The FM image shows a spherical morphology with bright red emission upon excitation with blue light (λ = 460–495 nm, Fig. 2c). The size and smooth surface of **MS$_{silk}$** is preferred for efficient light confinement.

We applied the conventional weighting method and SEM observations to confirm the successful enzymatic hydrolysis of **MS$_{silk}$** (Fig. S2a). The hydrolysis of **MS$_{silk}$** proceeded well in water containing proteinase K, as determined from the SEM images, where the microparticles of **MS$_{silk}$** degraded and finally formed an irregular amorphous residue (Fig. S3). Consistently, the weight of the solid components gradually decreased with a reaction rate constant k of 9.2 x 10^{-3} h^{-1} (Fig. S2b). As a reference, we conducted the same experiments with protease XVI instead of proteinase K, and no obvious change in weight (k = 3.8 x 10^{-4} h^{-1}) or in appearance was observed in the SEM images (Fig. S2b and Fig. S3). This result is reasonable because **MS$_{silk}$** consists dominantly of crystalline domains, according to a previous report,[18] and protease XVI is known to be unable to hydrolyse the crystalline domains of silk proteins.[25]

Microscopic PL (μ-PL) spectroscopy (Fig. 1a) revealed that **MS$_{silk}$** works as a WGM resonator, in which the photoluminescence (PL) from Nile Red is confined and resonated. The emission band in the μ-PL spectrum of **MS$_{silk}$** featured periodic sharp peaks that overlapped with the broad spontaneous emission band from Nile Red (Fig. 3a). The peaks were assigned to the transverse electric (TE) and magnetic (TM) modes of WGM resonance. The slight difference in wavelength between the TE and TM modes originated from the direction of the polarization (see supporting information for precise mathematical descriptions). In a simple mathematical approximation, the two series of resonance mode wavelengths (λ) should satisfy the equation $1/\lambda = l(\pi\eta d)^{-1}$ (Eq. 1), where d is the diameter of **MS$_{silk}$**, η is the refractive index of silk, and l is an integer. As expected from Eq. 1, the plot of $1/\lambda$ shows two series of linear relationships with λ (inset of Fig. 3a), each of which corresponds with the TE and TM modes. In addition, the η value (η = 1.57) calculated based on the slope of the plot coincides well with the reported value (η = 1.55 at approximately 600 nm), further supporting the WGM resonance.[26]

The light confinement property of **MS$_{silk}$** was maintained even in aqueous conditions. A drop of H_2O was carefully placed on the substrate, whereupon the μ-PL spectra of **MS$_{silk}$** sunk under water were measured by irradiating the excitation laser through the droplet. As shown in Fig. 3b, the emission band featured periodic resonance peaks, similar to those observed under atmospheric conditions (Fig. 3a). The peak broadening was attributed to the larger refractive index of H_2O (η = 1.33) than in air (η = 1.00) and the associated lower efficiency of light confinement inside the spheres. The peak positions and the spherical morphology of **MS$_{silk}$** were kept intact during the measurements (Fig. 3d), plausibly because the semicrystallinity of the silk provided sufficient stability under water.

The success in observing optical resonance peaks under water was attributed to the high light confinement efficiency of **MS$_{silk}$**. As a comparison, we synthesized red-fluorescent Nile Red-doped microspheres from potato starch, wheat starch and albumin proteins (**MS$_{potato}$**, **MS$_{wheat}$**, and **MS$_{albumin}$**, respectively, Fig. S4).[27, 28] The starch powders of potato and wheat were naturally microspherical and utilized for optical measurements after dying with Nile Red. **MS$_{albumin}$** was synthesized by using a modified mini-emulsion method. **MS$_{wheat}$** did not exhibit optical resonance in the PL spectra in an ambient atmosphere. **MS$_{potato}$**

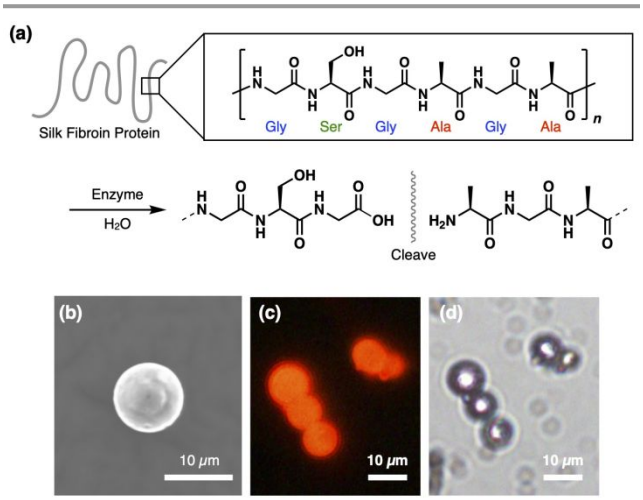

Fig. 2 (a) Schematic representation of the enzymatic hydrolysis of silk fibroin protein. (b–d) SEM, FM, and OM images of **MS$_{silk}$**.

and $\mathbf{MS}_{\mathbf{albumin}}$ exhibited periodic resonant peaks in the PL spectra in an ambient atmosphere, but the peak sharpness was lower than that of $\mathbf{MS}_{\mathbf{silk}}$. The resonance peaks of $\mathbf{MS}_{\mathbf{potato}}$ and $\mathbf{MS}_{\mathbf{albumin}}$ were blurred under water and were invisible spectroscopically due to the high refractive index of water relative to air. Thus, we chose $\mathbf{MS}_{\mathbf{silk}}$ for the further optical measurements described hereafter.

The hydrolysis reaction of silk fibroin proteins by the enzyme was successfully monitored with the time-course change in the μ-PL spectra of $\mathbf{MS}_{\mathbf{silk}}$. Prior to the μ-PL measurements, 30 μg of $\mathbf{MS}_{\mathbf{silk}}$ was incubated in pure water (1 mL), dried under ambient atmosphere, and then mixed with an aqueous solution of proteinase K (2.6 μg mL^{-1}), at which time (t) was defined as 0. The spectral position of the resonance peaks of $\mathbf{MS}_{\mathbf{silk}}$ remained virtually intact until t = 30 min with a slight shift towards a longer wavelength region (*vide infra*). After that, all resonance peaks shifted towards a shorter wavelength synchronously (Fig. 3c and 3d). This spectral change was reproducible with two other $\mathbf{MS}_{\mathbf{silk}}$. The blueshift of the resonance peaks was attributed to the decrease in the diameter of $\mathbf{MS}_{\mathbf{silk}}$ by the enzymatic hydrolysis reaction. Actually, $\mathbf{MS}_{\mathbf{silk}}$ that had sunk under deionized water without enzymes did not result in an obvious change in peak position (Fig. 3d). Analogously, no detectable change was observed with $\mathbf{MS}_{\mathbf{silk}}$ sunk in an aqueous solution of Protease XIV (30 μg mL^{-1}, Fig. 3d).

The reaction kinetics were calculated based on the spectral shift. Given that the peak shift ($\Delta\lambda$) was much smaller than the wavelength of the peak (λ), the relative change in volume (V/V_0) of a spherical resonator at a given t was determined according to the equation $V/V_0 = 1 - 3\Delta\lambda/\lambda$ (Eq. 2, see supporting information for the details of the equations), where V_0 represents the initial volume of $\mathbf{MS}_{\mathbf{silk}}$.[24, 29, 30] The exponential fitting of the plot in Fig. 3d provides the hydrolysis reaction rate k as 16 x 10^{-3} h^{-1} according to Eq. 2. The k value was larger than that obtained by the weighting method (k = 9.2 x 10^{-3} h^{-1}), which was attributed to the fragmentation of silk. The fragmentation decreased the size of the individual $\mathbf{MS}_{\mathbf{silk}}$ and affected the optical resonance peak position. In contrast, in the weighting method, the fragment was still included in the weight and not detected as weight loss.

Of note, the standard deviation (σ) of V/V_0 calculated based on the spectral shift was below 9 x 10^{-4}, which is considerably smaller than the σ observed with the weighting method (Fig. S2b), which ranges from 0.02 to 0.22, demonstrating the excellent precision of the μ-PL method. Moreover, the amount of the sample used to obtain a single data point with an error bar was significantly smaller (30 μg) than that used for the weighting method (30 mg). This feature is particularly valuable for biological research, where enzymes or substances are costly and scarce. We also confirmed that the doped dye did not affect the hydrolysis reaction. To assess the effect, we synthesized a microsphere ($^{\mathbf{MSB}}\mathbf{MS}_{\mathbf{silk}}$) doped with the blue fluorescent dye 1,4-bis(2-methylstyryl)benzene. The resonance peaks in the μ-PL spectra of $^{\mathbf{MSB}}\mathbf{MS}_{\mathbf{silk}}$ immersed in an enzymatic dispersion were blueshifted (Fig. S5). The reaction kinetics calculated based on the spectral change (15 x 10^{-3} h^{-1}) are comparable to those observed for $\mathbf{MS}_{\mathbf{silk}}$ (16 x 10^{-3} h^{-1}), confirming that the effect of the doped dyes on the protein structure and the enzymatic reaction is negligible.

The μ-PL method is applicable to measurements at an elevated temperature. An aqueous droplet containing $\mathbf{MS}_{\mathbf{silk}}$ and proteinase K was heated with a plate heater placed beneath the quartz substrate. The temperature was adjusted by using a thermocouple integrated into the heater. At every temperature tested (25, 30, and 45 °C), $\mathbf{MS}_{\mathbf{silk}}$ exhibited WGM resonance in the μ-PL spectra and a peak shift in the presence of proteinase K. The reaction rate k calculated based on the spectral shift increased from 16 x 10^{-3} to 97 x 10^{-3} h^{-1} as the temperature increased from 25 to 45 °C (Fig. 3e). The accelerated enzymatic activity at elevated temperatures observed with the μ-PL measurements was consistent with previous reports showing a monotonic and linear increase in the activity of proteinase K as a function of temperature up to 50–60 °C.[31, 32]

Our method was also advantageous with respect to the time resolution as well as the weight precision. As described above, the spectral peaks in Fig. 3d exhibited a slight redshift until t = 30 min. The spectral trend was reproducible and was not an artefact judging from the error bar. An analogous increase in the weight or volume of the substances in the early stage of enzymatic hydrolysis reactions was previously reported by another research group conducting QCM measurements with a thin organic film.[11] They attributed the increase to the

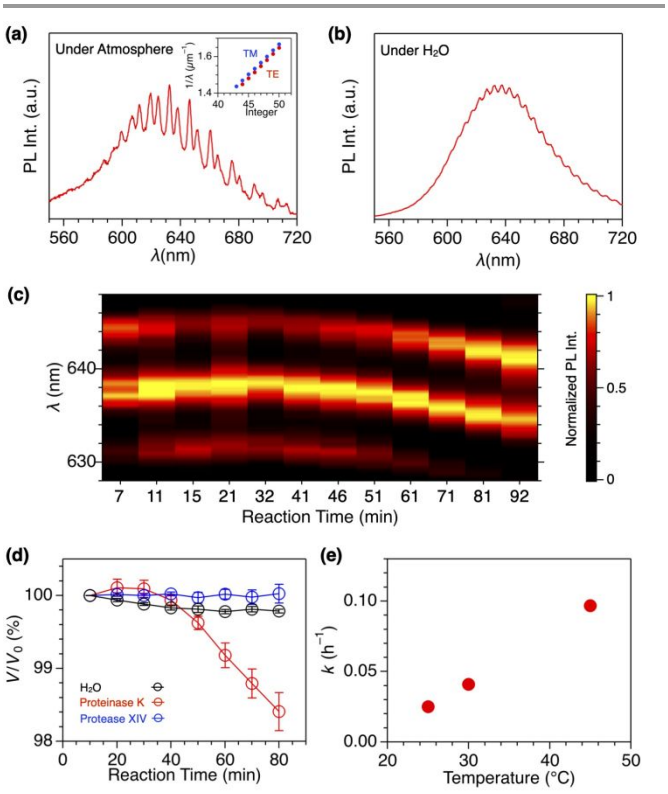

Fig. 3 (a, b) μ-PL spectra of $\mathbf{MS}_{\mathbf{silk}}$ put under atmosphere (a) and H_2O (b). The inset shows a plot of $1/\lambda$ for TE (red) and TM (blue) peak series as a function of integer. (c) A time-course profile of *in situ* μ-PL spectra observed with $\mathbf{MS}_{\mathbf{silk}}$ incubated in an aqueous solution of Proteinase K. (d) A plot of V/V_0 of $\mathbf{MS}_{\mathbf{silk}}$ versus the incubation time under H_2O (black), and aqueous solutions of proteinase K (blue) and protease XIV (red). (e) A plot of the kinetic constants of the hydrolysis reaction of $\mathbf{MS}_{\mathbf{silk}}$ as a function of reaction temperature.

adsorption of the enzymes onto the surface. Adsorption takes place in the early stage of the reaction. Subsequently, the enzymes unfold the polymers, which takes a certain interval. These two chemical steps resulted in the time lag observed in the time-course profile in the μ-PL spectra. As shown in Fig. S2b, the conventional weighting method could not detect these chemical steps due to the low prescription weight and the time-consuming analytical processes. In contrast, the spectral and time resolution of our μ-PL method was high enough to assess the change in volume and the lag time. The time resolution could be accelerated up to 0.05 sec, which is the minimum acquisition time of our spectrometer. Moreover, our method was intrinsically compatible with microscopic observations, which is a clear difference from QCM, probe microscopy, or other analytical methods.

In conclusion, we have established a microscope-compatible spectroscopic technique to analyse the catalytic and enzymatic hydrolysis reactions of water-insoluble natural fibroin polymers under *in situ* conditions. The change in mass of the polymer can be directly monitored as a spectral shift of the optical resonance peaks. The precision and time resolution of our method are high enough to trace the details of hydrolysis reactions. This method is not applicable to the late stage of the hydrolysis reaction because particles become too small to confine visible light. Nonetheless, the spectral profile in the initial and middle stages of the reaction is highly valuable for precisely analysing the reaction kinetics and for assessing the inherent catalytic activity of enzymes and the biodegradability of polymers.

Research groups that will benefit from this method include biochemical companies that develop enzymes for degradation and fermentation of polymers and molecular biologists who study phagocytosis and digestion. Our method enables fast and precise screening of the catalytic activity of an enzyme, which will accelerate the analysis and development of novel enzymes in industry. Our method is also applicable to hydrolysis inside a biological cell. Phagocytosis is one of the major targets in this case. The precise kinetic analysis of phagocytosis is a formidable challenge because it is a microscopic reaction and should be observed *in situ* with a microscope. Our method can fulfil these requirements. The integration of these micro-optical proves with other optical and electric devices for medical usages will also be of practical value.[33] Altogether, we believe our method will accelerate the future investigation of catalysts and enzymes and will contribute to further developments in biochemistry.

Conflicts of interest

The authors declare the following competing financial interest(s): A.T., H. Y., and Y.Y. are listed as inventors on a Japanese patent application (No. 2022-037340).

Notes and references

1. L. P. Walker and D. B. Wilson, *Bioresour. Technol.*, 1991, **36**, 3-14.
2. R. S. Flannagan, V. Jaumouille and S. Grinstein, *Annu. Rev. Pathol.*, 2012, **7**, 61-98.
3. Y. Sun and J. Cheng, *Bioresour. Technol.*, 2002, **83**, 1-11.
4. F. Talebnia, D. Karakashev and I. Angelidaki, *Bioresour. Technol.*, 2010, **101**, 4744-4753.
5. T. Ahmed, M. Shahid, F. Azeem, I. Rasul, A. A. Shah, M. Noman, A. Hameed, N. Manzoor, I. Manzoor and S. Muhammad, *Environ Sci Pollut Res Int*, 2018, **25**, 7287-7298.
6. S. Bahl, J. Dolma, J. Jyot Singh and S. Sehgal, *Mater. Today Proc.*, 2021, **39**, 31-34.
7. S. Lyu, J. Schley, B. Loy, D. Lind, C. Hobot, R. Sparer and D. Untereker, *Biomacromolecules*, 2007, **8**, 2301-2310.
8. A. K. Andrianov and A. Marin, *Biomacromolecules*, 2006, **7**, 1581-1586.
9. M. A. Sabino, S. Gonzalez, L. Marquez and J. L. Feijoo, *Polym. Degrad. Stab.*, 2000, **69**, 209-216.
10. V. Piemonte and F. Gironi, *J. Polym. Environ.*, 2012, **21**, 313-318.
11. X. Turon, O. J. Rojas and R. S. Deinhammer, *Langmuir*, 2008, **24**, 3880-3887.
12. T. M. Mohona, N. Dai and P. C. Nalam, *Langmuir*, 2021, **37**, 14214-14227.
13. P. Giunchedi, B. Conti, S. Scalia and U. Conte, *J. Control. Release*, 1998, **56**, 53-62.
14. C. F. van Nostrum, T. F. J. Veldhuis, G. W. Bos and W. E. Hennink, *Polymer*, 2004, **45**, 6779-6787.
15. F. Codari, S. Lazzari, M. Soos, G. Storti, M. Morbidelli and D. Moscatelli, *Polym. Degrad. Stab.*, 2012, **97**, 2460-2466.
16. K. Igarashi, A. Koivula, M. Wada, S. Kimura, M. Penttila and M. Samejima, *J. Biol. Chem.*, 2009, **284**, 36186-36190.
17. Y. Yamamoto, *Polym. J.*, 2016, **48**, 1045-1050.
18. W. Y. Heah, H. Yamagishi, K. Fujita, M. Sumitani, Y. Mikami, H. Yoshioka, Y. Oki and Y. Yamamoto, *Mater. Chem. Front.*, 2021, **5**, 5653-5657.
19. G. Q. Wei, X. D. Wang and L. S. Liao, *Laser Photon. Rev.*, 2020, 2000257.
20. L. He, Ş. K. Özdemir and L. Yang, *Laser Photon. Rev.*, 2013, **7**, 60-82.
21. A. Chiasera, Y. Dumeige, P. Féron, M. Ferrari, Y. Jestin, G. Nunzi Conti, S. Pelli, S. Soria and G. C. Righini, *Laser Photon. Rev.*, 2010, **4**, 457-482.
22. A. N. Oraevsky, *Quantum Electronics*, 2002, **32**, 377-400.
23. A. Qiagedeer, H. Yamagishi, M. Sakamoto, H. Hasebe, F. Ishiwari, T. Fukushima and Y. Yamamoto, *Mater. Chem. Front.*, 2021, **5**, 799-803.
24. N. Tanji, H. Yamagishi, K. Fujita and Y. Yamamoto, *ACS Appl. Polym. Mater.*, 2022, **4**, 1065-1070.
25. O. Haske-Cornelius, A. Pellis, G. Tegl, S. Wurz, B. Saake, R. Ludwig, A. Sebastian, G. Nyanhongo and G. Guebitz, *Catalysts*, 2017, **7**, 287.
26. G. Perotto, Y. J. Zhang, D. Naskar, N. Patel, D. L. Kaplan, S. C. Kundu and F. G. Omenetto, *Appl. Phys. Lett.*, 2017, **111**, 103702.
27. V. D. Ta, Y. Wang and H. Sun, *Adv. Opt. Mater.*, 2019, **7**, 1900057.
28. Y. Wei, X. Lin, C. Wei, W. Zhang, Y. Yan and Y. S. Zhao, *ACS Nano*, 2017, **11**, 597-602.
29. M. Gao, C. Wei, X. Lin, Y. Liu, F. Hu and Y. S. Zhao, *Chem. Commun.*, 2017, **53**, 3102-3105.
30. J. Ward and O. Benson, *Laser Photon. Rev.*, 2011, **5**, 553-570.
31. K. Yazawa, M. Sugahara, K. Yutani, M. Takehira and K. Numata, *ACS Catalysis*, 2016, **6**, 3036-3046.
32. Y. Ren, H. Luo, H. Huang, N. Hakulinen, Y. Wang, Y. Wang, X. Su, Y. Bai, J. Zhang, B. Yao, G. Wang and T. Tu, *Int. J. Biol. Macromol.*, 2020, **154**, 1586-1595.
33. T. Yan, Z. Li, F. Cao, J. Chen, L. Wu and X. Fang, *Adv. Mater.*, 2022, **34**, 2201303.